Tribol Lett (2017) 65:40
DOI 10.1007/s11249-017-0823-y

ORIGINAL PAPER

Tribological Performance and Lubrication Mechanism of Alumina Nanoparticle Water-Based Suspensions in Ball-on-Three-Plate Testing

Anshun He[1] · Shuiquan Huang[1] · Jung-Ho Yun[2] · Hui Wu[3] · Zhengyi Jiang[3] · Jason Stokes[2] · Sihai Jiao[4] · Lianzhou Wang[2] · Han Huang[1]

Received: 17 November 2016 / Accepted: 30 January 2017 / Published online: 9 February 2017

Abstract The lubrication performance of alumina (Al_2O_3) nanoparticle water-based suspensions was systematically investigated using a ball-on-three-plate testing configuration with alloy steel on stainless steel contact. The size and concentration of Al_2O_3 nanoparticle were varied to obtain optimal performance. The effects of testing load, sliding speed and contact surface roughness on the lubrication performance of the Al_2O_3 suspensions were investigated. It was found that 1 to 2 wt.% 30 nm Al_2O_3 nanoparticle suspensions showed up to 27% friction and 22% wear reduction, in comparison with water glycerol solution. Under different testing conditions, the suspensions also showed noticeably more stable and improved tribological performance. Wear mark analysis revealed that during tribological testing the nanoparticles formed a layer of dynamically balanced tribo-thin film, preventing the direct contact between asperities of alloy steel ball and stainless steel plate. The nanoparticles were also believed to fill up the trenches of the plate surface through mending effect and carry the wear debris induced in running-in period to avoid abrasive wear.

✉ Han Huang
han.huang@uq.edu.au

[1] School of Mechanical and Mining Engineering, The University of Queensland, Brisbane, QLD 4072, Australia

[2] School of Chemical Engineering, The University of Queensland, Brisbane, QLD 4072, Australia

[3] School of Mechanical, Materials and Mechatronic Engineering, University of Wollongong, Wollongong, NSW 2522, Australia

[4] Research Institute (R&D Center), Baoshan Iron & Steel Co., Ltd., Shanghai 201900, China

Keywords Alumina · Nanoparticle · Nano-scale friction · Water-based · Ball-on-three-plate

1 Introduction

Lubrication has been a long standing issue in many industrial applications as it can significantly affect the wear, as well as energy consumption of machineries [1]. Over the decades, oil and oil-based emulsion lubricants were widely used to reduce wear and friction between a contact pair. The balanced viscosity and shear strength of oil-based lubricants enable the separation of the contact pair through a film dynamically formed during sliding. In such cases, friction regime is shifted from solid/boundary friction to mixed and hydrodynamic lubrication [2]. Despite their widespread applications, oil-based lubricants do have some drawbacks such as toxicity and non-biodegradable nature.

As a consequence, a great research effort was directed towards developing water-based lubricants [3]. In addition to its environment-friendly and low-cost nature, water-based lubricants demonstrated excellent desirable properties for tribological applications, such as high burning resistance, and high heat conductivity [4]. However, water by itself cannot provide satisfactory lubricating performance in some applications because of its inherent problems, e.g. low viscosity, corrosion, and low boiling point [5, 6]. In order to improve the water-based lubricant performance, additives including various chemical compounds and particulate solids were often used [7]. Some nano-sized particles and platelets were demonstrated to be effective additives to improve the tribological performance of water-based lubricants. For example, laminated structure nanomaterials, such as h-BN and graphene oxide, can be stably

dispersed in water, and they have been shown to enhance wear resistance and reduce coefficient of friction [8, 9]. The drawbacks are that these lubricants are typically difficult to synthesis, and they tend to have poor thermal stability for high-temperature tribological applications. Metal materials such as Cu, Fe and Co were reported to significantly reduce the coefficient of friction characterised by four ball testing using Cr6 bearing steel balls [10, 11]. However, those metallic nanoparticles are difficult to disperse in water [12].

Metallic oxide nanoparticles, such as TiO_2, Fe_2O_3, ZnO, CeO_2 and Al_2O_3, have demonstrated promising properties as additives for water-based lubricants. The nanoparticles are typically thermally stable with superb heat conductivity [9, 12–18], and their dispersing stability in water can be handily improved through mechanical mixing and addition of nontoxic surfactants [15, 16]. Nevertheless, the role of nanoparticles in tribological performance is still not well understood. For instance, Radice et al. [16] found Al_2O_3 nanoparticles could reduce the coefficient of friction by 40–50% and the wear rate by one order of magnitude for a stainless steel plate to alumina ball contact. In contrast, Gara et al. [12] compared the tribological performance of ZnO and Al_2O_3 nanofluids using a steel-to-steel ball-on-disc testing configuration, and found that Al_2O_3 possessed anti-friction properties, but could not reduce wear. Compared with ZnO, Al_2O_3 nanoparticles produced more significant wear because of its much higher hardness. Apparently, the mechanism and tribological performance of Al_2O_3 water-based nanofluids need to be further clarified.

In this work, we report a systematic tribological study of the Al_2O_3 nanoparticle water-based lubricants using a ball-on-three-plate tester. The effects of nanoparticle size, concentration, testing speed, load and contact roughness on the tribological performance were comprehensively investigated. By use of wear mark analysis, the lubrication mechanism of Al_2O_3 nanoparticle suspensions for alloy steel on stainless steel contact was revealed.

2 Experiments

2.1 Al_2O_3 Nanoparticle Suspensions

Al_2O_3 nanoparticles of 30, 150, and 500 nm in diameter were used in this study, which are commercially available (supplied by Yurui Chemical Co. Ltd, China). The morphology of the nanoparticles was examined using a transmission electron microscopy (JEM2100, JEOL, Japan). Figure 1a–c shows the TEM images of the three Al_2O_3 nanoparticles, respectively. As shown in Fig. 1a, the 30-nm particles have uniform size distribution, and the particle shapes are quite spherical. The shapes of 150 and 500 nm nanoparticles are less spherical, exhibiting irregular morphologies. Figure 1d shows the representative XRD spectra of Al_2O_3 nanoparticle, indicating that the particles have crystal structure of α-a trigonal (R-3c), which was formed via thermal dehydroxilation at above 1300 °C.

The concentration of Al_2O_3 nanoparticles being studied in this work ranged from 0.2 to 8 wt.%, which is generally believed to be the effective range of nanoparticle suspensions for lubrication applications [19]. Glycerol is often used in water-based lubricants as a viscosity modifier, which is safe to human body and environmental friendly. Different content (up to 10 wt.%) of glycerol was added to investigate its effect on tribological performance of the suspension. The abbreviation, Gly, was used in the graphs to represent the addition of 10 wt.% glycerol to water. To disperse nanoparticles into water uniformly, ultrasonic probe (Branson Digital Sonifier 450, USA) was used to mechanically deagglomerate Al_2O_3 nanoparticles. A high-intensity ultrasonic agitation of 400 W was applied for 10 min with a 5-s on/off interval. Circulated chilling water bath was used to maintain suspension temperature during the agitation process. The synthesised nanoparticle suspensions were found to be stable without sedimentation over 3 days, after which the dispersions could be restored to their original status by ultrasonic bathing for 5 min. Water with 10 wt.% glycerol solution was used as a bench mark for comparison.

2.2 Ball-on-Three-Plate Tests

Figure 2a shows the Modular Compact Rheometer (or MCR, Anton Paar, Austria) with a tribological ball-on-three-plate testing module, and Fig. 2b is the close view of the ball-on-three-plate set-up. As shown in Fig. 2c, the upper ball is placed on the three lower plates with a pre-set normal load applied. The lower plates are fixed, forming 45° to the rotating axis and the plate holder is suspended so that the plates can be centred when a normal load is applied. During testing, the ball rotates in contact with the fixed lower plates, and the torque experienced by the rotating ball was recorded. The specifications of the balls and plates are shown in Table 1. The as-received plates have an average roughness of 292 ± 87 nm, measured by a stylus profiler (DektakXT Stylus Profiler, Bruker, USA). To investigate the effect of roughness, the plates were also lapped to have the roughness values of 206 ± 27 and 37 ± 6 nm. The sliding speed was varied from 20 to 100 mm/s, and the normal load was changed from 10 to 40 N, which corresponds to a Hertzian contact pressure of 645 MPa to 1.02 GPa. The total sliding distance of 7.5 m was kept the same for all the tests. Prior to tribological testing, both balls and plates were ultrasonically cleaned in acetone for 10 min. The ball and plate were replaced after

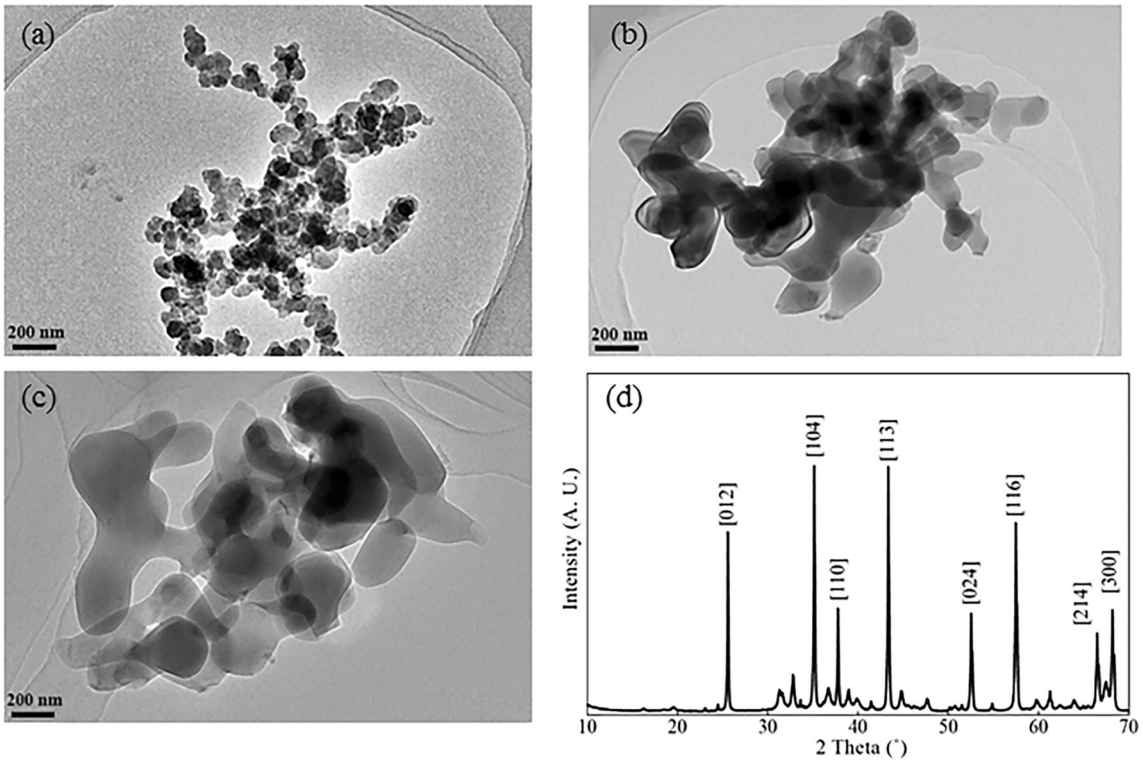

Fig. 1 TEM images of Al_2O_3 nanoparticles with average sizes of **a** 30, **b** 150, and **c** 500 nm; **d** the XRD spectrum of the 30 nm Al_2O_3 nanoparticles

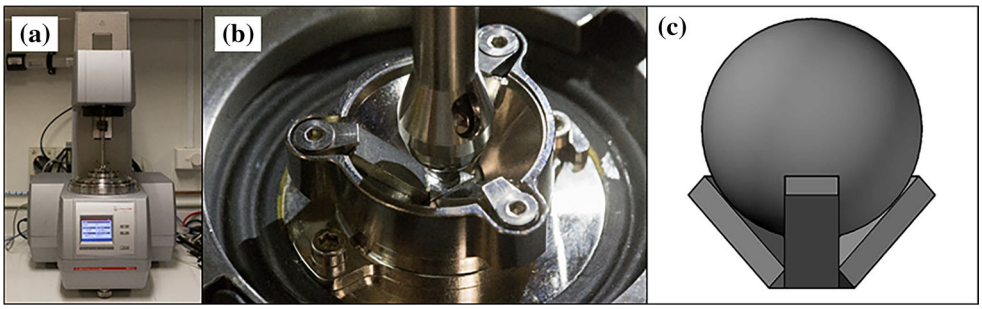

Fig. 2 **a** Front view of a ball-on-three-plate tester; **b** upper ball hovering over the plates and plate holder; **c** schematic illustration of the testing configuration

Table 1 Specifications of the balls and plates used in ball-on-three-plate tests

	Material	Surface treatment	Surface roughness (nm)
Ball	AISI 52100 alloy steel	Lapped	11.1 ± 0.4
Plate	AISI 304 stainless steel	Milled	270.7 ± 18.7
		#120 lapped	206.2 ± 27.6
		#1200 lapped	37.0 ± 6.2

each test to maintain the same experimental context. Each test was repeated three times and the results were averaged.

2.3 Wear Mark Analysis

After testing, the lower plates were cleaned ultrasonically in acetone for 5 min to remove any loose debris and excessive nanoparticles. The wear marks on the plates were measured by use of a laser confocal microscope (LEXT OLS4100, Olympus, Japan). The wear surfaces were examined using a field emission scanning electron microscope (FE-SEM, JSM-7001F, JEOL, Japan). The elemental study on selected spots and mapping was performed by use of energy-dispersive X-ray (EDS) analysis.

3 Results and Discussion

3.1 Characteristics of Tribological Testing

Figure 3 shows the coefficient of friction (COF) time histories, represented by the COF-distance curves. The results were obtained from the tribological tests at 50 mm/s and 40 N with no lubrication (i.e. dry condition), 2 wt.% Al_2O_3 suspension and water glycerol solution. Under the dry condition, the COF increased to a significantly high value of above 0.8 at the beginning of testing, which fluctuated considerably. The test was terminated earlier than the others because very loud noise and strong vibration were generated. When water and Al_2O_3 suspension were used, at the initial stage over a travel distance of 1.5 m, the COF was relatively high as severe asperity contact occurred and material removal took place, which is commonly known as the running-in period [20, 21]. After the running-in period ended, COF became quite stable, which was almost irrelevant to the distance being used in this test.

The wear mark sizes were measured at the distances of 0.75, 1.5, 4.5 and 7.5 m, respectively. Figure 4 shows the wear mark radii for all the tests. Without lubrication, the wear rate was high, with the wear mark radius increased to 317 μm in the 3-m test. In comparison, for the lubricated cases, the running-in period was observed approximately in the beginning distance of 1.5 m. During this period, the wear mark radius increased significantly to above 100 μm due to the severe asperity contact. After running-in, for water glycerol solution the wear reached the stable status quickly, and the wear mark radius increased gradually from 137 to 167 μm over the 6-m testing distance. However, for the 2 wt.% Al_2O_3 suspension, the wear mark sizes remained almost at the same level of 120 μm with distance, in line with the COF (Fig. 3). Similar phenomenon was reported in the previous study on the lubrication of oxide nanoparticles [17].

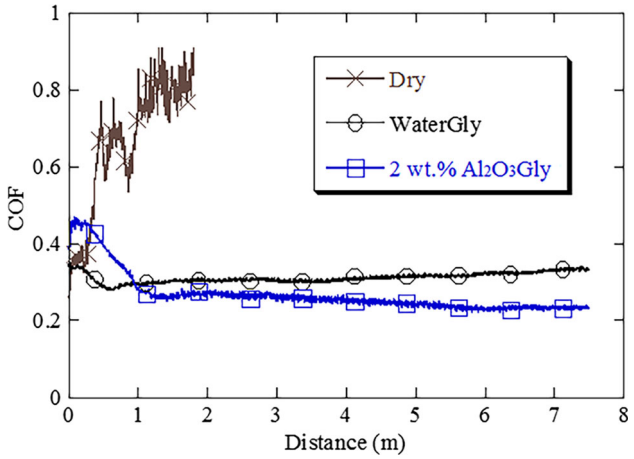

Fig. 3 COF–distance curves of tribological tests using 2 wt.% Al_2O_3 suspension and water glycerol solution, compared with dry condition

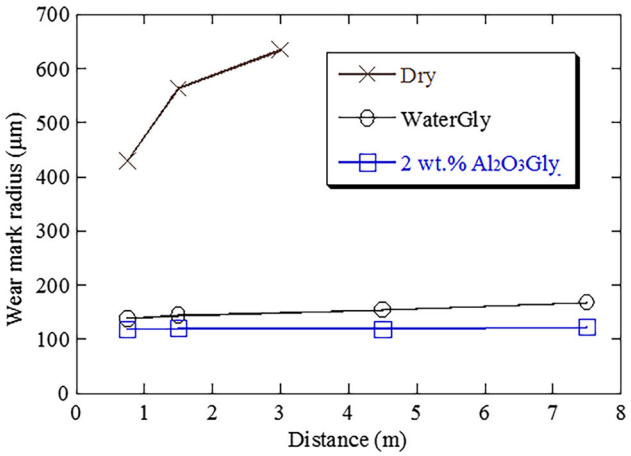

Fig. 4 Wear mark radius at different testing distances of tribological tests using 2 wt.% Al_2O_3 suspension and water glycerol solution, compared with dry condition

3.2 Effect of Glycerol

Figure 5 shows the effect of glycerol, which was added into water and 2 wt.% Al_2O_3 suspension, on COF and wear

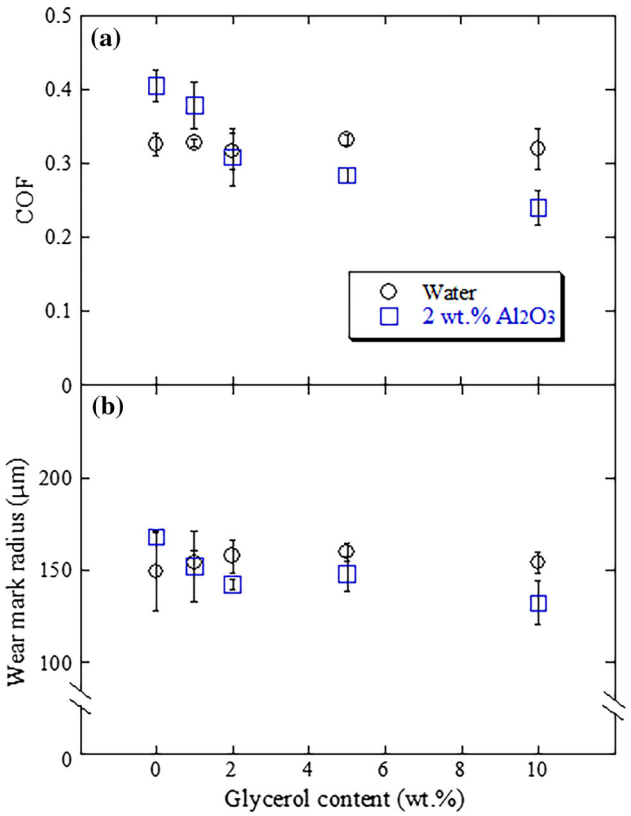

Fig. 5 Effect of glycerol content on **a** COF and **b** wear mark radius yielded by water and 2 wt.% Al_2O_3 suspension

mark radius. The addition of glycerol into pure water showed little effect on COF and wear mark size. The COF and wear mark radius remained almost constant at 0.322 ± 0.006 and 155.1 ± 3.6 μm for all the glycerol contents, respectively. The increase in glycerol content in water would increase the viscosity of the solution and its wettability to the steel surface slightly. However, such a change in viscosity and wettability did not make significant effect on the lubrication performance under the current testing condition.

The glycerol content in the Al_2O_3 nanoparticle suspension did make impact on the lubrication performance. As shown in Fig. 5, the increase in glycerol content from 0 to 10 wt.% resulted in substantial decrease in both COF (from 0.4 to 0.24) and wear mark radius (from 167.9 to 132.1 μm), though the decrease in wear size became insignificant when the glycerol content was over 2 wt.%. When the glycerol content exceeded 2 wt.%, the Al_2O_3 suspension showed lower COF and smaller wear mark radius than that of the solvent. This is because Al_2O_3 nanoparticle surfaces adsorbed glycerol, and the hydroxyl group on glycerol thus improved the nanoparticle-steel adhesion.

3.3 Effect of Particle Size and Concentration

Three different Al_2O_3 nanoparticles of 30, 150 and 500 nm in diameter were used for examining the size effect. They were dispersed in water with 10 wt.% glycerol. The tests were performed under a normal load of 40 N and a sliding speed of 50 mm/s. Figure 6 shows the COF–distance curves obtained from the tribological tests. The curve of water glycerol solution was also plotted in the figure for comparison. The COF curves appear quite stable across the entire travel distance. It should be noted that in this figure only the last 2.5 m of COF values were collected, to remove the effect of the running-in period. As shown in Fig. 6, the smaller the particle size used, the smaller the COF was induced, with the water glycerol solution producing the highest COF.

Figure 7 shows the averaged COF and wear mark radii obtained from the tests with the Al_2O_3 nanoparticle water-based lubricants with different particle sizes and concentrations. Note that "0%" concentration refers to the water glycerol solution. It is clear that with the addition of Al_2O_3 nanoparticles into water the lubricants showed lower COF and smaller wear marks than the water glycerol solution. It is seen in Fig. 7a that the decrease in COF with the increasing particle concentration almost reached the minimum at 2 wt.%, and further increase in concentration did not reduce the COF. Similarly, as shown in Fig. 7b, the wear mark radius decreased with the increase in concentration to 1 wt.%, and further increase resulted in a slight

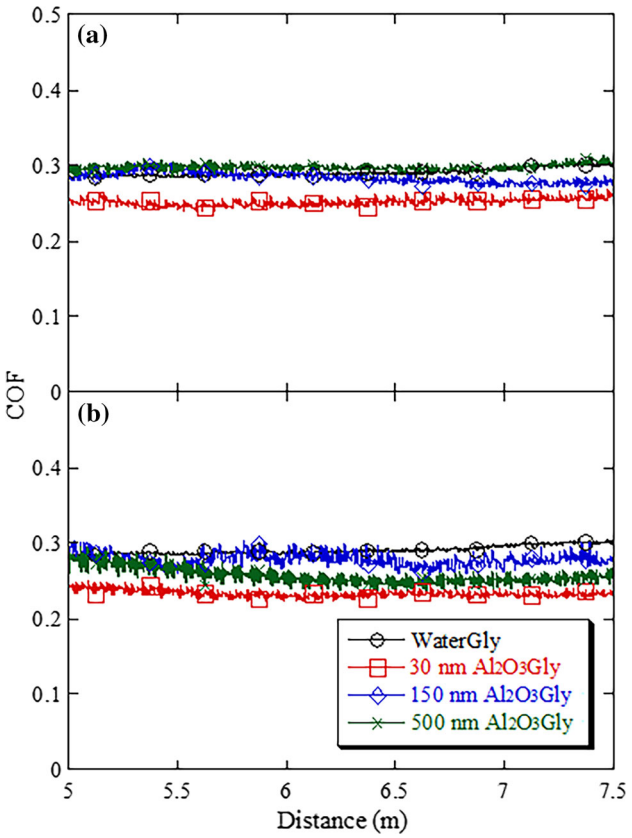

Fig. 6 COF–distance curves of **a** 1 wt.%, and **b** 2 wt.% Al_2O_3 suspensions with averaged particle sizes of 30, 150, and 500 nm. For comparison, water glycerol solution was used as a benchmark

increase in wear mark size. Apparently, particle concentration had an optimal value in terms of lubrication performance. If too little, nanoparticles were insufficient for making effective entrainment, but if too much, the suspension became excessively dense, which might cause agglomeration and unnecessary abrasive wear. In this case, concentrations of 1 and 2 wt.% Al_2O_3 nanoparticles with 30-nm particle size appeared appropriate; therefore, these two suspensions were selected in the further study.

3.4 Effect of Testing Conditions

Figure 8 shows the effect of normal load on the COF and wear mark radius using 1 and 2 wt.% Al_2O_3 suspensions and water glycerol solution. The sliding speed was kept at 50 mm/s. For all the tested conditions being used, COF was not affected by the change of normal load. Overall, 2 wt.% Al_2O_3 suspension showed the lowest averaged COF of 0.23, which was 27% reduction compared to that of water glycerol solution. The 1 wt.% Al_2O_3 suspension showed slightly higher COF (0.27) than the 2 wt.% one. As seen in Fig. 8b, the wear mark radius increased with the increase in normal load for all tested conditions. This is as expected

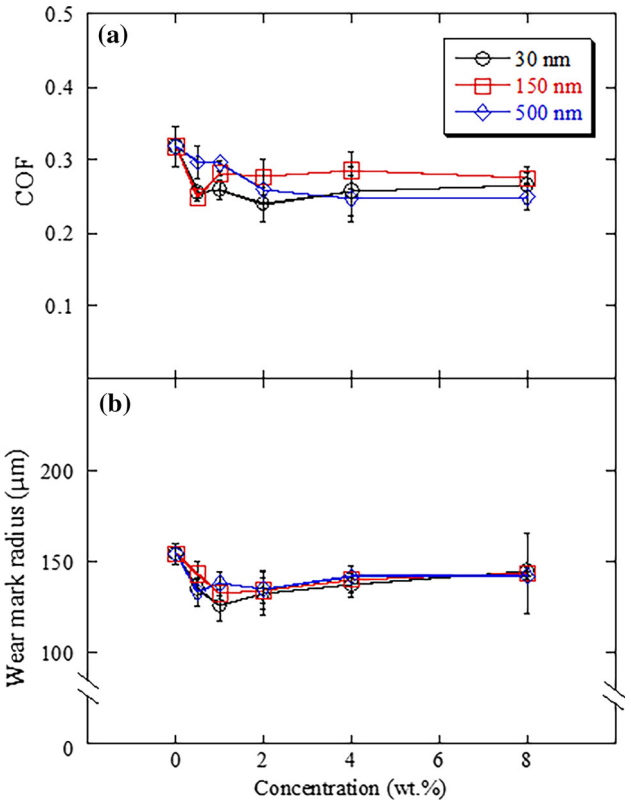

Fig. 7 Effect of Al_2O_3 concentration and size on **a** COF and **b** wear mark radius in comparison with water glycerol solution

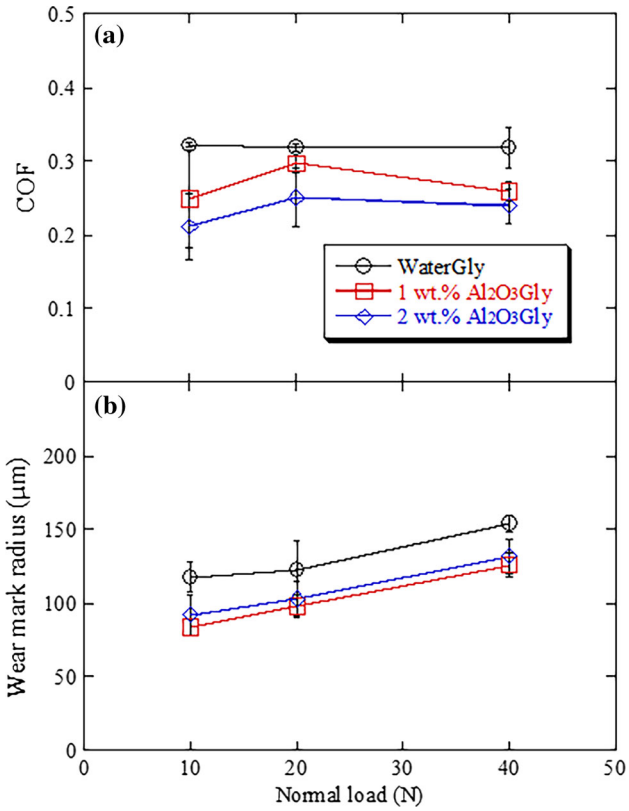

Fig. 8 Effect of normal load on **a** COF and **b** wear mark radius obtained from the tribological tests using 1, 2 wt.% Al_2O_3 suspensions, and water glycerol solution

because at a constant speed, a higher load can increase the contact pressure and result in more material removal. However, the wear mark sizes from Al_2O_3 suspensions were significantly smaller than that obtained using water glycerol solution at all tested loads. The averaged wear mark radius reduction was 22 and 17% for 1 and 2 wt.% Al_2O_3 suspensions, respectively. This indicates that the Al_2O_3 suspensions enhanced the tribological performance within the tested normal load range.

Figure 9 shows the effect of sliding speed on the COF and wear mark radius for a constant normal load of 40 N being used. For all the tested conditions, the COF decreased with the increase in sliding speed. With the water glycerol solution, the COF decreased slightly by 9.5% when the speed was increased from 25 to 100 mm/s. The decrease was more prominent by 20 and 24% for the 1 and 2 wt.% Al_2O_3 suspensions, respectively. As shown in Fig. 9b, the wear mark at a low speed of 25 mm/s for water glycerol solution was large (205 μm in radius). Then, it was reduced to a smaller area of about 160 μm in radius at 50 and 100 mm/s. The effect of sliding speed on wear mark radius was less obvious for Al_2O_3 suspensions. For the tested speed range, the averaged wear mark radii for 1 and 2 wt.% Al_2O_3 suspensions were 133 and 134 μm, respectively. The trend of COF and wear mark radius of water glycerol solution appears to agree with the famous Stribeck curve [22], in which the decrease in sliding speed can change the lubricating regime from mixed to boundary lubrication. Given that the same lubricant and contact load were used, the decrease in speed would decrease the Sommerfeld number [23], thus resulting in a smaller contact separation and hence a larger COF and wear mark. However, during the tribological test after running-in, the Al_2O_3 nanoparticles could enter the contact area, which thus improved tribological performance even at a small sliding speed. Therefore, in this case, the wear mark radius was kept very small for all tested speeds being used.

3.5 Effect of Plate Roughness

Figure 10 shows the effect of the plate roughness on the COF and wear mark radius. It can be seen that when Al_2O_3 suspensions were used, the surface roughness of the lower plate had insignificant effect on both COF and wear mark size. When water glycerol solution was employed, the increase in plate roughness from 37 to 206 nm had little influence on the COF and wear mark radius, but the roughness increase from 206 to 270.7 nm led to significant decrease in both COF and wear mark size. This is because

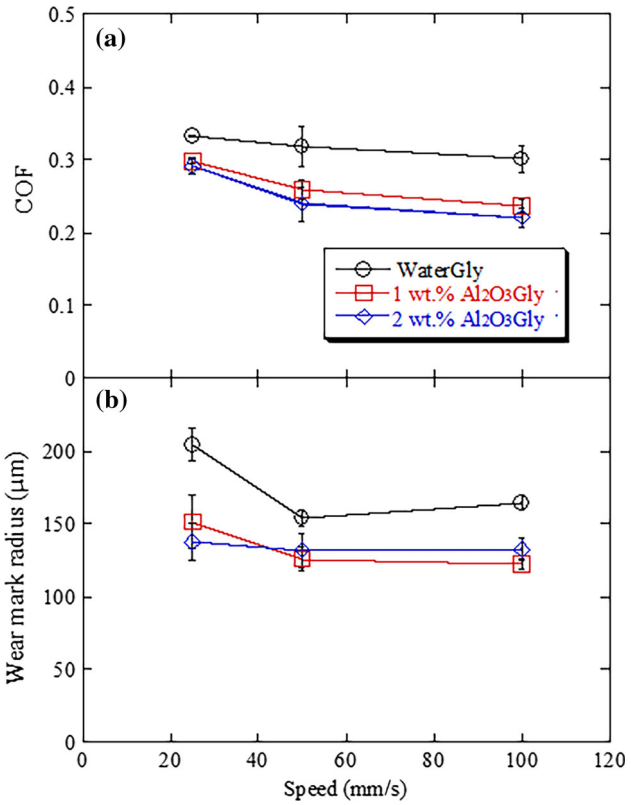

Fig. 9 Effect of sliding speed on **a** COF and **b** wear mark radius obtained from the tribological tests using 1, 2 wt.% Al_2O_3 suspensions, and water glycerol solution

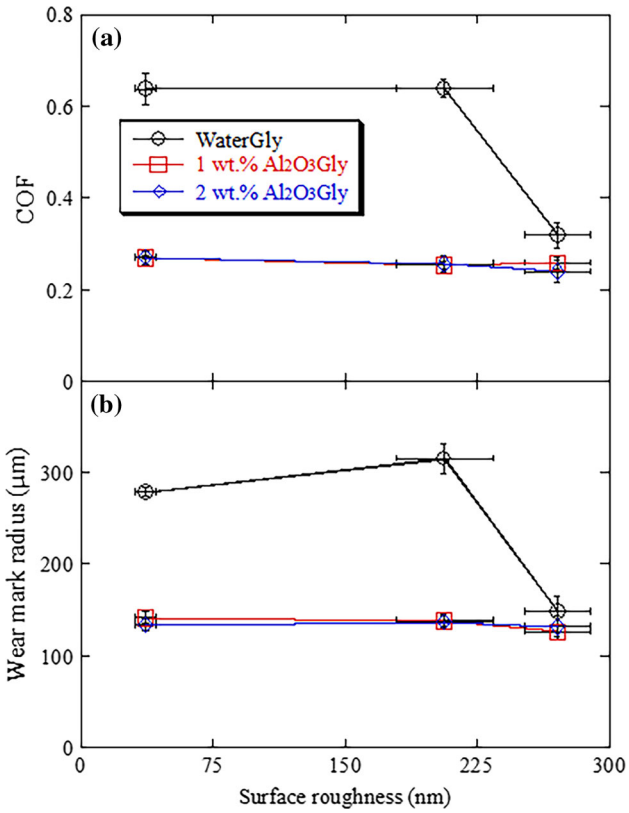

Fig. 10 Effect of surface roughness of the lower plate on **a** COF, and **b** wear mark radius obtained from the tribological tests using 1, 2 wt.% Al_2O_3 suspensions, and water glycerol solution

when the plate surface is rough, the grooves on the surface might serve as reservoirs and retain water, which thus improve the lubrication performance, leading to significantly lower COF and wear mark size.

However, when Al_2O_3 suspensions were used, the nanoparticles played a dominant role in lubrication through separating the ball and the plate. Even with relatively smooth plate surfaces, nanoparticles were able to form a tribo-film over the contact interface, producing the improved lubrication performance [12, 24, 25].

3.6 Surface Characteristics of Wear Marks

FE-SEM images of the wear mark surfaces obtained from the tests using water glycerol solution and 1 wt.% Al_2O_3 suspension after 1.5 m of the running-in period are shown in Fig. 11. For water glycerol solution, ploughing grooves were clearly seen, as shown in Fig. 11a, indicating the occurrence of severe adhesive wear [23]. The corresponding EDS spectrum shown in Fig. 11d indicated that the wear mark had the same composition as that of stainless steel. For Al_2O_3 suspension, it can be seen in Fig. 11b that some particles were observed on the surface. The back scattered imaging of the same location (Fig. 11c) and the subsequent elemental analysis (see Fig. 11f) suggested that those particles are Al_2O_3. This indicates that nanoparticles were embedded onto the steel substrate under high initial contact pressure during running-in. At the later stage, those particles could take effect and separate the steel-to-steel contact to reduce wear.

Figure 12 shows the SEM images and EDS oxygen Kα1 peak mappings of the wear marks obtained from the tests using water glycerol solution and 1 wt.% Al_2O_3 suspension at the travel distance of 7.5 m. The oxygen mapping of Fig. 12a is shown in Fig. 12c, where straight marks were found aligned to the sliding direction (indicated by the white arrow) when water glycerol solution was used. This strongly suggests that adhesive wear and localised oxidation occurred. Different from the water glycerol solution, the wear mark surface from the test using the Al_2O_3 suspension was smooth without adhesive wear grooves, as shown in Fig. 12b. The aluminium mapping shown in Fig. 11d indicated that the majority of Al_2O_3 nanoparticles was accumulated on the entrance side of the contact, where the majority of contact pressures were located. Some nanoparticles were also found being trapped in the existed trenches, which was not aligned with the sliding direction. This observation indicated that during stable wear period,

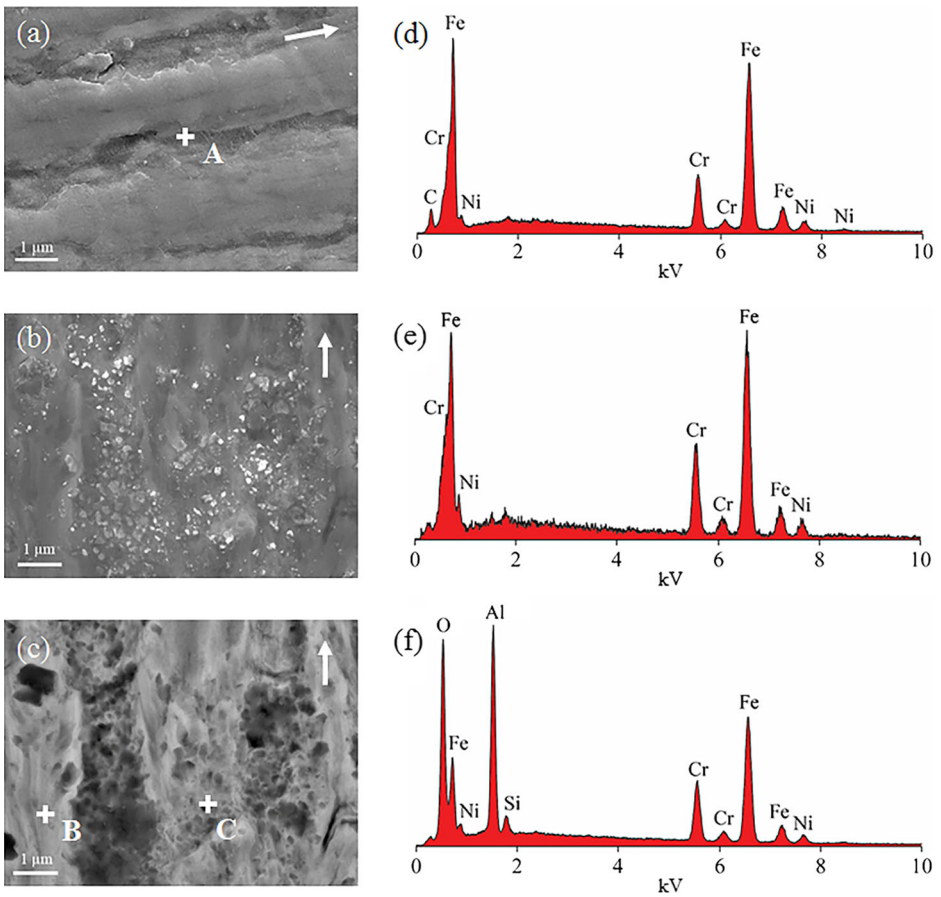

Element	Weight (%)
C	3.83
Cr	13.97
Fe	74.90
Ni	7.30
Total	100.00

Element	Weight (%)
Cr	18.66
Fe	72.11
Ni	9.23
Total	100.00

Element	Weight (%)
O	11.92
Al	12.43
Si	1.08
Cr	14.70
Fe	54.15
Ni	5.72
Total	100.00

Fig. 11 FE-SEM secondary electron images of wear mark surface after 1.5 m tests with **a** water glycerol solution, and **b** Al_2O_3 suspensions; **c** back scattered image of **b**; **d**, **e** and **f** are the point elemental analysis of Point *A*, *B* and *C*, respectively

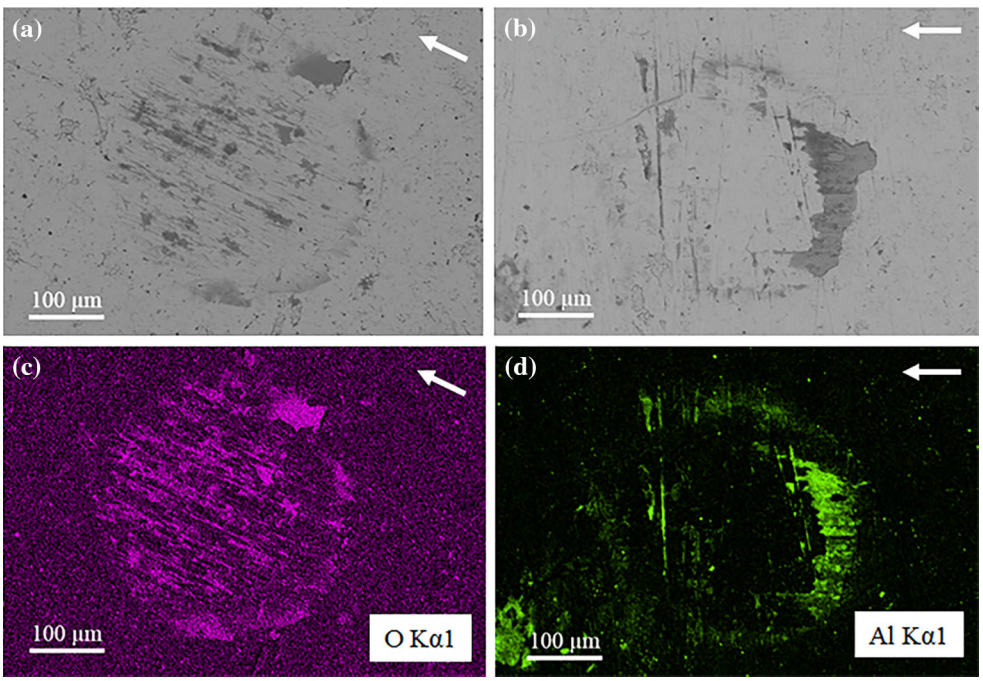

Fig. 12 SEM backscattered electron images of wear mark surface after 7.5-m tests using **a** water glycerol solution, and **b** Al_2O_3 suspension; **c** oxygen mapping on **a**, and **d** aluminium mapping on **b**. The white arrows indicate the sliding direction

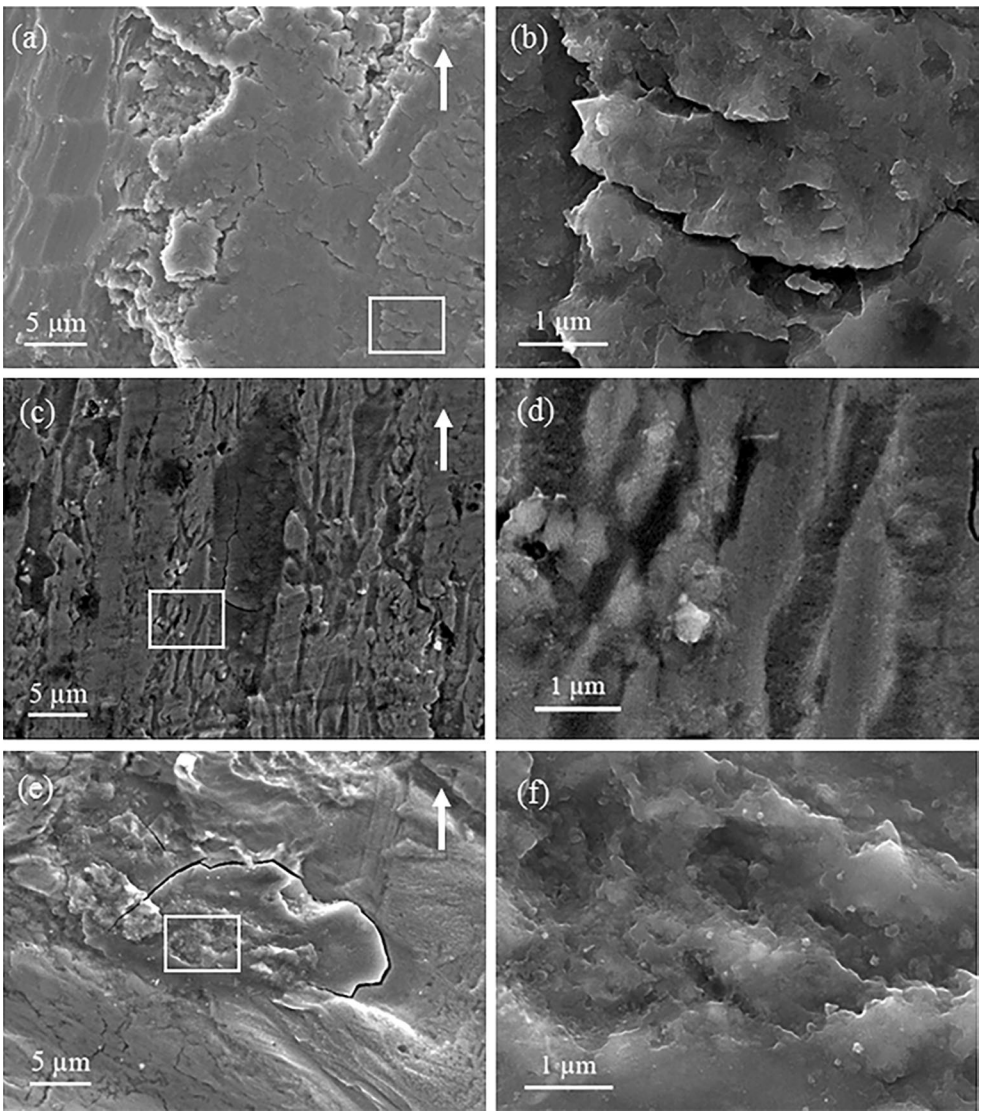

Fig. 13 FE-SEM images of wear mark surfaces on the lower plates after 7.5-m tests under **a**, **b** dry condition, **c**, **d** lubrication by water glycerol solution, and **e**, **f** lubrication by Al_2O_3 suspensions. The *white arrows* indicate the sliding direction, and the enlarged images were taken from the corresponding white rectangles

the Al_2O_3 particles might re-enter the contact area and continue to provide lubrication.

Figure 13 shows the detailed morphologies of the wear mark surfaces obtained at the travel distance of 7.5 m under dry condition, using water glycerol solution, and 1 wt.% Al_2O_3 suspension. For dry condition, repeated wave-like patterns were observed, as shown in Fig. 13a. The wave-like patterns were formed most likely by the coupling effect of contact vibration and work hardening of steel. The other distinct feature was through-thickness cracks. Leaf-like residues were also found in the enlarged image of Fig. 13a, and Fig. 13c–d shows the wear surfaces lubricated by the water glycerol solution. Grooves were found being aligned to the sliding direction, as indicated by the white arrow in Fig. 13c. Those grooves are the evidence of asperity contact and severe adhesive wear via plastic deformation [23]. Micro-cracks were occasionally found on the wear mark surface, suggesting that brittle oxide might be formed on the steel substrate. Figure 13e, f shows the wear surfaces lubricated by the 1 wt.% Al_2O_3 suspension. The wear surface was quite smooth in comparison with the surface shown in Fig. 13c, and adhesive wear grooves were no longer found. A micro-crack was found on the surface, as shown in Fig. 13e. Al_2O_3 nanoparticles appeared being embedded onto the wear mark surface, as shown in Fig. 13f.

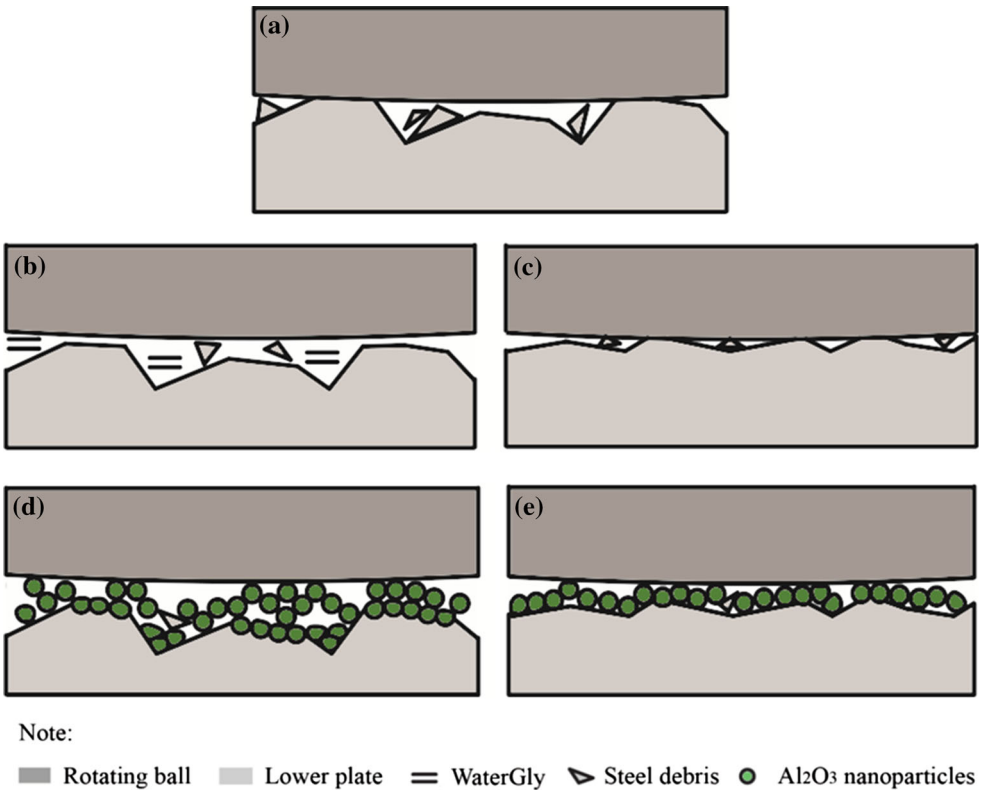

Fig. 14 Schematic illustrations of the contacts **a** with dry condition; with lubrication using the water glycerol solution on the plates of relatively **b** high and **c** low roughness; and with lubrication using Al_2O_3 water suspension on the plates of relatively **d** high and **e** low roughness

4 Discussion on the Lubrication Mechanism of Al_2O_3 Suspensions

Based on the analysis above, the lubrication mechanism of water-based Al_2O_3 suspensions can be summarised. The schematics of the contact during the tribological tests with the developed lubricants in comparison with those of the dry condition and the water glycerol solution are shown in Fig. 14.

For dry condition, severe asperity contact occurred, and the debris removed from the steel substrate remained in the contact area, as shown in Fig. 14a. This resulted in vibration and caused work hardening on the contacted region of the steel substrate. Therefore, the debris from these regions acted like third-body abrasives and caused scratches.

When the water glycerol solution was used, a small portion of the debris resulted from the asperity contact during running-in period were carried away by the water flow, but some might still be stored in the trenches on the steel surface, as shown in Fig. 14b, c. Water glycerol might still be retained in the trenches of the surface when the plate roughness was relatively high, as shown in Fig. 14b, but no water could be kept on the surface if the plate was relatively smooth, as shown in Fig. 14c. Under the condition of Fig. 14b, the water glycerol in the trenches could effectively separate the contact between the ball and the plate. However, for the case shown in Fig. 14c, asperity contact between ball and plate was predominant. Therefore, the increase in plate roughness could result in significant decreases in COF and wear mark area, as shown in Fig. 10.

When the Al_2O_3 water suspension was used, Al_2O_3 nanoparticles played multiple roles in the lubrication. During the running-in period, some nanoparticles were embedded on the plate surface, acted as a load bearer. Those nanoparticles could form tribo-films on both rough and smooth plate surfaces shown in Fig. 14d, e, preventing the ball from direct contact with the plate. During the stable wear period, most nanoparticles re-entered the contact area and the replenishment and loss of nanoparticles between the contact surfaces could reach a dynamic balance. The dynamic lubricant flow also took away the steel debris from the plate caused by asperity contact. The rest of the nanoparticles entering the contact could fill up the existed trenches on the surface and "recover" the surface via the so-called "mending" effect [26]. Tribo-sintering occurred, and nanoparticles were compressed to form islands in the trenches. As a result, the COF maintained at a relatively low level, and the wear after running-in period was effectively minimised. As long as nanoparticles could completely separate the ball and the plate, variation of plate roughness would have insignificant effect on the lubrication performance characterised by COF and wear mark area, as shown in Fig. 10.

5 Conclusions

The lubrication performance of water-based Al_2O_3 nanoparticle suspensions was investigated systematically. The effects of the testing conditions and the size and concentration of nanoparticles in the suspensions were revealed. With the water glycerol solution being used as lubricants, the decrease in plate roughness resulted in significantly increased COF and wear mark radius due to the loss of water reservoirs on the plate surface. With the Al_2O_3 water suspension, noticeably more stable and improved tribological performance was obtained, regardless of plate roughness. In particular, the 1 and 2 wt.% 30 nm Al_2O_3 nanoparticle suspensions gave the lowest COF and the smallest wear mark, up to 27 and 22% reduction, respectively, in comparison with that of the water glycerol solution.

The role of Al_2O_3 nanoparticles in the water-based suspension was revealed. During running-in, the nanoparticles were embedded into the steel substrate and acted as load bearer. After running-in, Al_2O_3 nanoparticles effectively separated the contact between the ball and the plate through forming a dynamically balanced tribo-thin film. The steel debris could also be mixed into the suspension, consequently, significantly reducing abrasive and adhesion wear. The Al_2O_3 nanoparticles also filled up the existed trenches on the surface and reduced the friction through mending effect.

Acknowledgements The authors would like to acknowledge the financial supports from Baosteel under project BA13012 and Australia Research Council (ARC) through Linkage Project (LP150100591). This work was performed in part at the Queensland node of the Australian National Fabrication Facility (ANFF). ASH would like to acknowledge The University of Queensland (UQ) for the UQI Scholarship and the technical support and assistance from Dr. Heather Shewan. JRS acknowledges support from ARC Discovery Project DP150104147, and he acknowledges that the tribology-fixture used in this study is on loan from Anton Paar.

References

1. Yoshizawa, H., Chen, Y.L., Israelachvili, J.: Fundamental mechanisms of interfacial friction 1. Relation between adhesion and friction. J. Phys. Chem. **97**(16), 4128–4140 (1993)
2. Schmid, S.R., Wilson, W.R.D.: Lubrication mechanisms for oil-in-water emulsions. Lubr. Eng. **52**(2), 168–175 (1996)
3. Gao, Y.J., Chen, G.X., Oli, Y., Zhang, Z.J., Xue, Q.J.: Study on tribological properties of oleic acid-modified TiO_2 nanoparticle in water. Wear **252**(5–6), 454–458 (2002)
4. Peng, Y.T., Hu, Y.Z., Wang, H.: Tribological behaviors of surfactant-functionalized carbon nanotubes as lubricant additive in water. Tribol. Lett. **25**(3), 247–253 (2007)
5. Lei, H., Guan, W.C., Luo, J.B.: Tribological behavior of fullerene-styrene sulfonic acid copolymer as water-based lubricant additive. Wear **252**(3–4), 345–350 (2002)
6. Bowden, F.P., Tabor, D.: Friction and Lubrication. Methuen, London (1960)
7. Tomala, A., Karpinska, A., Werner, W., Olver, A., Störi, H.: Tribological properties of additives for water-based lubricants. Wear **269**(11), 804–810 (2010)
8. Cho, D.H., Kim, J.S., Kwon, S.H., Lee, C., Lee, Y.Z.: Evaluation of hexagonal boron nitride nano-sheets as a lubricant additive in water. Wear **302**(1–2), 981–986 (2013)
9. Liu, Y.H., Wang, X.K., Pan, G.S., Luo, J.B.: A comparative study between graphene oxide and diamond nanoparticles as water-based lubricating additives. Sci. China Technol. Sci. **56**(1), 152–157 (2013)
10. Padgurskas, J., Rukuiza, R., Prosycevas, I., Kreivaitis, R.: Tribological properties of lubricant additives of Fe, Cu and Co nanoparticles. Tribol. Int. **60**, 224–232 (2013)
11. Wu, Y.Y., Tsui, W.C., Liu, T.C.: Experimental analysis of tribological properties of lubricating oils with nanoparticle additives. Wear **262**(7–8), 819–825 (2007)
12. Gara, L., Zou, Q.: Friction and wear characteristics of water-based ZnO and Al_2O_3 nanofluids. Tribol. Trans. **55**(3), 345–350 (2012)
13. Zhao, C.L., Chen, Y.K., Ren, G.: A study of tribological properties of water-based ceria nanofluids. Tribol. Trans. **56**(2), 275–283 (2013)
14. Phuoc, T.X., Massoudi, M.: Experimental observations of the effects of shear rates and particle concentration on the viscosity of Fe_2O_3-deionized water nanofluids. Int. J. Therm. Sci. **48**(7), 1294–1301 (2009)
15. Gu, Y., Zhao, X.C., Liu, Y., Lv, Y.X.: Preparation and tribological properties of dual-coated TiO_2 nanoparticles as water-based lubricant additives. J. Nanomater. **2**, 1–8 (2014)
16. Radice, S., Mischler, S.: Effect of electrochemical and mechanical parameters on the lubrication behaviour of Al_2O_3 nanoparticles in aqueous suspensions. Wear **261**(9), 1032–1041 (2006)
17. Kato, H., Komai, K.: Tribofilm formation and mild wear by tribosintering of nanometer-sized oxide particles on rubbing steel surfaces. Wear **262**(1–2), 36–41 (2007)
18. Murshed, S.M.S., Leong, K.C., Yang, C.: Enhanced thermal conductivity of TiO_2-water based nanofluids. Int. J. Therm. Sci. **44**(4), 367–373 (2005)
19. Mosleh, M., Atnafu, N.D., Belk, J.H., Nobles, O.M.: Modification of sheet metal forming fluids with dispersed nanoparticles for improved lubrication. Wear **267**(5–8), 1220–1225 (2009)
20. Xu, J.G., Kato, K., Hirayama, T.: The transition of wear mode during the running-in process of silicon nitride sliding in water. Wear **205**(1–2), 55–63 (1997)
21. Chen, M., Kato, K., Adachi, K.: The difference in running-in period and friction coefficient between self-mated Si_3N_4 and SiC under water lubrication. Tribol. Lett. **11**(1), 23–28 (2001)
22. Lu, X., Khonsari, M., Gelinck, E.: The Stribeck curve: experimental results and theoretical prediction. J. Tribol. **128**(4), 789–794 (2006)
23. Hersey, M.D.: Theory of lubrication. Wiley, New York (1938)
24. Novak, C., Kingman, D., Stern, K., Zou, Q., Gara, L.: Tribological properties of paraffinic oil with nanodiamond particles. Tribol. Trans. **57**(5), 831–837 (2014)
25. Lee, K., Hwang, Y., Cheong, S., Choi, Y., Kwon, L., Lee, J., Kim, S.H.: Understanding the role of nanoparticles in nano-oil lubrication. Tribol. Lett. **35**(2), 127–131 (2009)
26. Liu, G., Li, X., Qin, B., Xing, D., Guo, Y., Fan, R.: Investigation of the mending effect and mechanism of copper nano-particles on a tribologically stressed surface. Tribol. Lett. **17**(4), 961–966 (2004)